Bulgarian Chemical Communications, Volume 50, Special Issue A (pp. 108 - 113) 2018

Application of inkjet printing technology for SOFCs anode fabrication and modification

R.I. Tomov[1*], A. Fakeeh[1], T.B. Mitchell-Williams[1], M. Krauz[2], R.V. Kumar[1], B.A.Glowacki[1,3]

[1] *Department of Materials Science and Metallurgy, University of Cambridge, United Kingdom*
[2]*Institute of Power Engineering - Ceramic Department CEREL, Poland*
[3] *Institute of Power Engineering, Warsaw, Poland*

Received September 25, 2017; Accepted October 17, 2017

Feasibility of inkjet printing technology for fabrication and modification of SOFC electrodes and electrolytes was studied. Drop on demand inkjet printing offers fast, scalable and cost efficient processing path by reproducibly dispensing droplets in the range of *nL* to *pL* volumes at high rates (*kHz*) and high velocity (*1-10 m/s*). Electromagnetic print heads were utilized to dispense droplets of various inks (doped ceria, Ni oxide) on demand. Printing parameters including pressure, nozzle opening time were studied in order to optimize the inks jetting and delivery. Reduction of SOFC anode polarization losses was pursued via infiltration nano-engineering of the electrode's scaffolds. Two - step fabrication using inkjet printing was implemented. In the first step porous electrode scaffolds (Gd:CeO_2-NiO) were created by printing suspension inks. During the second step inkjet printing infiltration was utilized for controllable loading of Gd:CeO_2 nano-decorations on the scaffolds. Anode symmetrical cells were characterized by Electrochemical Impedance Spectroscopy in order to reveal the relation between the surface nano-structure and the electrochemical performance. Electrochemical impedance spectroscopy measurements confirmed a significant reduction and convergence of the area specific resistance (ASR) values for infiltrated anodes with different NiO/Gd:CeO_2 volume ratios. This work demonstrated the feasibility of achieving significant improvements in SOFC electrodes performances via simple industrially scalable procedure.

Keywords: inkjet printing, infiltration, nano decoration, doped ceria

INTRODUCTION

A combination of geopolitical, economic and environmental concerns regarding the depletion of fossil fuels reserves and global warming have been driving forces behind considerably renewed interest in fuel cell technologies. Fuel cells (FCs) offer direct electrochemical conversion of the energy into electricity and heat without efficiency limitations inherent to heat engines governed by the Carnot cycle. Demonstrated high electrical efficiencies can substantially exceed those typical for coal-fired power plants [1]. FCs can be scaled across a wide range of sizes - from systems with outputs as small as 1 W to facilities operating in MW range. Nickel is commonly used as anode material due to its high catalytic activity for fuel oxidation, high electrical conductivity and mechanical/ chemical compatibility with traditional ion conductive electrolytes [2]. The commercial anodes are based on cermet compositions like NiO–YSZ (yttrium stabilized zirconia) or NiO-Gd:CeO_2 (GDC) consisting of three different phases - metallic Ni, ion conductive ceramic and percolating pores acting as fuel and reactants diffusion pathways. The mixture of Ni and ion conductive phase in the cermet provides an extension of three-phase boundary (TPB) and alleviates the thermal stresses caused by the difference of the thermal expansion coefficients (TECs) between NiO and electrolyte materials (TEC_{8YSZ}~10.4-11.0 $ppmK^{-1}$, TEC_{GDC}~12.7 $ppmK^{-1}$, TEC_{NiO} ~14.2 $ppmK^{-1}$) which is beneficial for withstanding stresses caused by rapid thermal cycling. The cermet materials also offer chemical and thermal stability in oxidizing and reducing atmospheres as well as good oxygen ionic conductivity over a wide range of conditions [3, 4]. Depending on the design Solid Oxide Fuel cells (SOFCs) can operate at various temperatures within the region of 500-1000^{o}C [5,6]. Adversely, at elevated temperatures the Ni phases in the cermet have a tendency to coarsen and agglomerate, reducing the TBP due to poor adhesion of metal to the ceramic material. Such deterioration at high operational temperatures as well as the high overall cost of production effectively inhibit commercialization of SOFC technology. Commonly sought solution is to lower the operating temperature to intermediate temperature (IT) range of 600–800^{o}C. Such low operating temperatures can suppress the TPB deterioration and significantly expand the choice of materials e.g. enable the use of less expensive stainless steel as interconnects and manifolds. However, because of the lower

* To whom all correspondence should be sent.
E-mail: rit21@cam.ac.uk.

temperature the overall performance of a SOFC system would decrease due to exponential increase in electrode polarization losses. It has been shown that infiltration of the SOFC electrodes (both anode and cathode) with ionic conductive phase is an effective method to develop nano-engineered electrode materials with high performance and stability at IT [7].

This study reports on the application of Inkjet Printing (IJP) for the fabrication and infiltration of NiO/Gd-CeO_2 (GDC) anodes with different ratio of the constituent phases. The IJP technique is simple and cost-effective non-contact "wet" technique for fabrication of ceramic coatings onto variety of surfaces which allows utilization of very thin fragile porous support (ceramic or metal). It can reproducibly dispense droplets in the range of nL volumes at high rates (kHz). Drop-on-demand (*DOD*) ceramic inkjet printing offers excellent thickness and uniformity control and introduces the possibility of printing 2D and 3D patterns as well as continuous coatings. Inkjet systems offers wide scale of application - from experimentation platforms working with customized inks, up to mass manufacturing systems that can print rapidly and competitively on industrial scale. The technology is cost effective and environmentally friendly through waste minimization of the expensive precursors. The influence of the major printing parameters and required optimization steps were explored for both suspension and sol-gel inks. The production of anodes and electrolyte coatings with a modified Domino print head was reported previously by Tomov et al. [8] using suspension inks. Wang et al. [9,10] deposited GDC electrolytes on NiO-8YSZ cermet anodes using sol–gel-based precursor solutions. Sukeshini et al. [11] employed a DMP-2831 printer for the deposition of 8YSZ electrolyte layers, LSM-YSZ and LSM cathode layers on to NiO–8YSZ supports, reporting a maximum power density of 450 mW/cm^2 at 850°C in hydrogen.

EXPERIMENTAL

Inks preparation

Electrolyte and electrode depositions as well as ionic phase (GDC) infiltrations were performed by an electromagnetically (EM) driven print head with 100 μm ruby nozzle orifice and X-Y planar positioning system. EM technology was chosen because it offers simplicity and reliability of use, as well as wider range of ink/suspension compatibility. The preparation of stable suspension and sol-gel inks is of critical importance for achieving repeatable jetting without clogging the nozzles. For the suspension inks commercial NiO, and GDC powders were mixed with alpha-Terpineol and binders, and ball milled with 3YSZ beads in 3YSZ bowls in a planetary mill. The mass load of the ceramic powders was limited by the rheological working window of the nozzles, which defined the regime of stable repeatable jetting. Hence, the viscosity of the suspension inks had to be adjusted by adding lower viscosity solvent – Methanol (MeOH). GDC precursor solution (1.5 M total metal concentration) was prepared by dissolving cerium (III) acetate hydrate (Sigma-Aldrich) and gadolinium (III) acetate hydrate (Sigma-Aldrich) in two steps in propionic acid (Sigma-Aldrich) under reflux for 4 hours at 120 °C. The solution was then cooled to room temperature and filtered through 0.3 μm polypropylene membrane syringe filter (Whatman) to eliminate possible contamination with dust particles. The precursor was further diluted to reduce the viscosity to a suitable level as determined by the print-head requirements. A number of different solvent/ precursor mixtures were tested to evaluate the stability of the ink, which was determined by observing precipitation levels after shelf storage for 24 hours. From the various solvents tested 1-propanol was selected as a diluting agent producing the most stable printable inks. The dilution at volume ratio 1:1 (precursor :solvent) was found suitable to produce stable jetting without observing any splashing effects. Jetting of all types of inks was optimized by drop visualization procedure with the aim to avoid formation of satellite drops at practical Weber and Reynolds numbers. The inks were filtered through 3 μm glass micro-fibre filters before being loaded into the nozzle compartments. The nozzles were observed to execute reproducible drop on demand tasks without clogging the internal fluidic pathways of the assembly.

Symmetrical cells fabrications

GDC powder, Hydroxypropyl cellulose and Ethanol were mixed and milled for 4 hours. Following evaporation of the solvent, the powder was uniaxially pressed into pellets with 12.5 mm diameter under 3 tonnes pressure. The pellets were sintered at a heating rate of 3°C min^{-1} to 900 °C and held for an hour. Anodes (NiO/GDC) with different constituents volume ratios (60:40 and 80:20 vol% ratio) suspension inks were printed on both sides of the GDC pellets and fired at 900 °C in air forming porous NiO/GDC anode scaffolds. An infiltration of the GDC sol ink was carried out by inkjet printing of ~8 nL drops as determined by drop visualisation in a reciprocal pattern on each side of the cell. Each infiltration step (per side) contained 368 drops (~3.2 μL of ink). A horizontal drop spacing of 0.6 mm was used to achieve an overlap of 25% between the drops surface replicas. Each printed

layer was allowed to drain and the absolute position of the print head was offset by 0.3 mm in the X and Y directions to avoid drop stacking. An intermediate heat treatment was applied after every second deposition, increasing the temperature from ~20 ºC to 300 ºC within 10 minutes. Such treatment led to the removal of the solvent from within the scaffold aiding further infiltration steps. Various infiltration-loading levels of GDC nanoparticles into the anode scaffold were achieved by varying the number of printing steps. Finally, as treated pellets were sintered at 1400 ºC for 4 hours in order to achieve fully dense electrolytes. As sintered symmetrical cell were ~0.5 mm thick and ~11 mm in diameter.

Characterization

Electrochemical impedance spectra (EIS) of the symmetrical cells were measured with the electrochemical interface and a frequency response analyser (Solartron 1260) under the open-circuit voltage (OCV) condition. Symmetrical cells were heated at 5 °C/min ramping rate to temperatures from 500 to 600 °C, and tested under Ar/4% H_2 in a frequency range of 1 MHz to 0.1Hz with AC amplitude of 10 mV. Silver mesh was painted to the electrodes in order to ensureconductivity along the surface of the electrodes.

RESULTS AND DISCUSSION

Drop visualisation

Drop visualisation was used to study the drop generation process for each combination of printing parameters (pressure and opening time) and, in conjunction with image analysis, to determine the corresponding drop velocity and drop volume. The greatest advantage of the drop visualisation system is that it allows rapid examination of whether the rheological condition of the ink is suitable for printing. Ideally, any ink should be tailored in such a way that each triggering event results in a single drop, without satellite drops, before reaching the substrate. Figure 1 shows jetting behaviour of GDC sol ink at optimized conditions where the initial drop breaks into a series of small drops after it detaches from nozzle, but the smaller drops then soon catch up with the main drop and form back to a single drop. Within the stable jetting regime, it was found that the drop volume was approximately 8 nL. The maximum velocity achieved in this case was ~ 2.2 m/s.

Infiltration effect

Multiple infiltrations were conducted by repeated inkjet-printing/low temperature calcinations. As seen in the high resolution SEM images shown in Figure 3, the NiO/GDC scaffolds

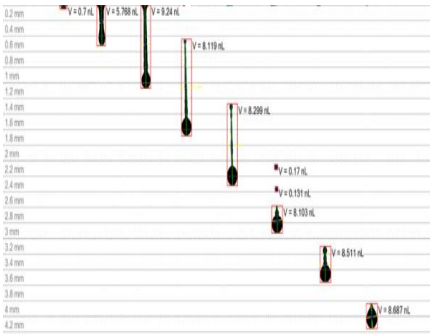

Fig.1. Montage of images from the drop visualisation showing optimized jetting of the GDC sol ink.

Anodes fabrication

Figure 2 presents tops surface SEM images of two blank (non-infiltrated) NiO/GDC anodes after high temperature sintering. The anode with 80:20 NiO/GDC ratio showed clear micro-cracking of the surface due to the difference in the TECs of the constituent phases. This was expected to lead to deterioration of both electronic and ionic conductive paths in the anode.

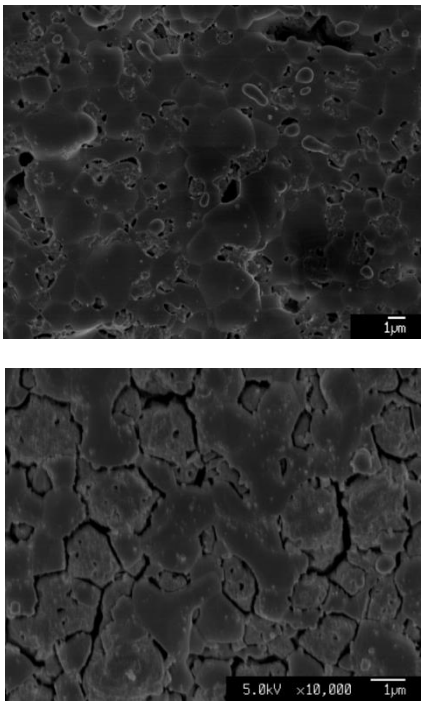

Fig. 2. SEM surface images of blank composite GDC:NiO anodes – (a) 60:40 NiO:GDC vol% ratio, and (b) 80:20 NiO:GDC vol% ratio

were composed of well-connected NiO and GDC grains with sizes ranging between 1 and 3 µm. After the infiltration, the scaffolds were uniformly decorated with GDC nanoparticles forming nano-scale sub-structures. All infiltrated samples showed

similar sub-structures with GDC nanoparticle size varying in the range of 50–200 nm. Remarkably, the infiltrated nano sub-structure was retained after the high temperature sintering at 1400 ºC. Similar observation was reported by Lee et al. [12] for Ni-GDC infiltration. The exact nature of this effect is not clear as according to Rupp et al. [13] self-limited grain growth for nano GDC characterized by grain boundary diffusion was observed for temperatures below 1100ºC. One could speculate that the retention of the nano sub-structure could be related to the strong bonding between the GDC nano particles and the micro-strain defects in the anode scaffold.

A quantitative confirmation of the effect of infiltration on the electrochemical performance was investigated by EIS. Comparison of the Nyquist plots of the reference blank anodes and infiltrated anodes (8 infiltrations) at 550 ºC is shown in Figure 4. The EIS spectra for all measured symmetrical cells were similar in shape, showing single arc associated with the activation polarization resistance (R_p) at the anode without clear separation between low and high frequency arcs.The total (R_t) and Ohmic (R_o) polarization resistances were estimated from the low and high frequency intercepts of the Nyquist plots with the real axis. R_p was calculated from the difference between these two values divided by two - $R_p = (R_t - R_o)/2$ in order to account for the symmetrical nature of the cells. The activation polarizations of samples with no infiltration corresponded to the ones derived from geometric model considerations published in the literature with 60:40 NiO/GDC scaffold showing significantly lower ASR than the 80:20 GDC scaffold (see Table 1). Despite the higher Ni content in the reduced anodes R_o of 80:20 anodes was found to be double the value of 60:40 anodes.

Table 1: .Impedance of samples with NiO:GDC of 60:40 and 80:20 with 0 and 8 infiltrations at 550˚C

	Rp, Ω cm^2		Ro, Ω	
Number of infiltrations	60:40	80:20	60:40	80:20
0	1.62	4.49	8.30	16.94
8	1.23	1.48	5.68	5.98

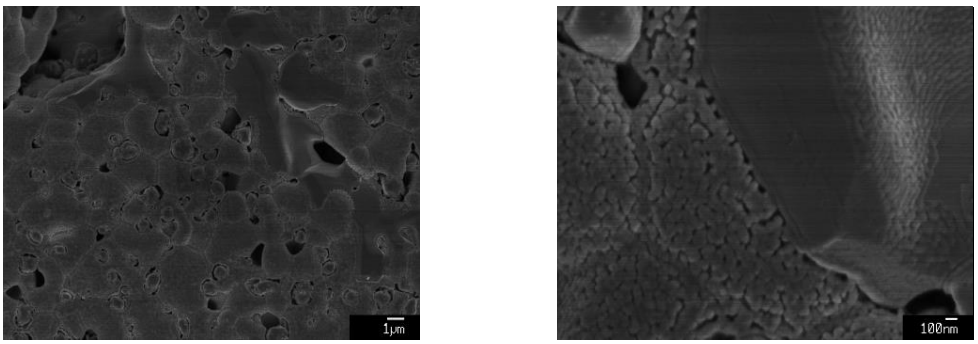

Fig. 3. NiO:GDC 60:40 scaffold nano-decorated with 8 infiltrations of GDC sol ink at increasing magnification

These deviations can be explained by the anode microstructure, which shows clear evidence of cracking for the 80:20 anode resulting from the TECs differences during high temperature sintering. Such cracking of the scaffold effectively resulted in local breakage of the ionic and electronic current paths and increase of R_o and R_p. Sharp decrease in R_p and R_o after the infiltration procedure was observed for both anode compositions converging in R_p values reaching 1.23 and 1.48 Ω cm^2 and R_o values reaching 5.68 and 5.98 Ω cm^2 at 550ºC. The promotion factors F_p and F_o were chosen as figures of merit defined as:

$$F_p = ASR_{ref} / ASR_{inf}$$
$$F_o = R_{o\text{-}ref} / R_{o\text{-}inf}$$

where ASR_{ref} was the area specific resistance of the reference anode (ASR=R_p x anode surface area) and the $R_{o\text{-}ref}$ was Ohmic resistance values of the reference (non-infiltrated) anode while ASR_{inf} and $R_{o\text{-}inf}$ were the ASR and Ohmic resistance values of the infiltrated anodes. The inset in Figure 4 shows the frequency dependence of the impedance imaginary part for different NiO/GDC ratios. It was obvious that the infiltration procedure led to reduction of high frequency losses commonly associated with the charge transfer reaction. The observed effect can be related to the increase of TPB via infiltration of GDC. As seen in Figure 5 the activation polarization resistance promotion factor F_p was substantially higher for 80:20 scaffold

compositions reaching maximum of 4.95 at higher temperature (600ºC). Note that F_p for 60:40 scaffold reached lower value of 2.27. The promotion factor for the Ohmic resistance F_o was also shown to be systematically higher for the 80:20 anode ranging between 2.65 and 2.75 within the measured temperature range. Comparing the data in Table 1 we can conclude that the infiltration procedure led to near equalisation the R_o and R_p values of the two anode composition investigated.

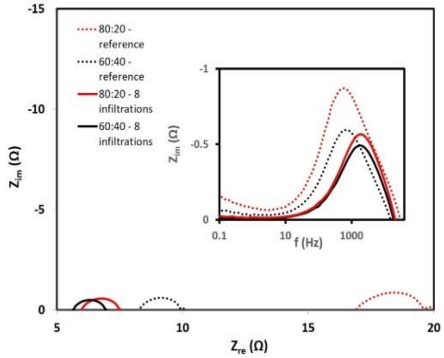

Fig. 4. EIS spectra of anodes with 0 infiltrations (reference) and 8 infiltrations at 550ºC

The insert shows the frequency dependence of the impedance imaginary part for different NiO/GDC ratios. This result indicated that both scaffolds reached similar lever of performance via infiltration and nano-decoration with ionic conductive GDC nanoparticles. The effect was due to the higher degree of TPB extension on Ni rich composition scaffold and cracks "healing" effect of the infiltrated GDC. The nano-decoration provided improved percolation more expressed at higher temperature where GDC was contributing to both ionic and electronic scaffold conductivity.

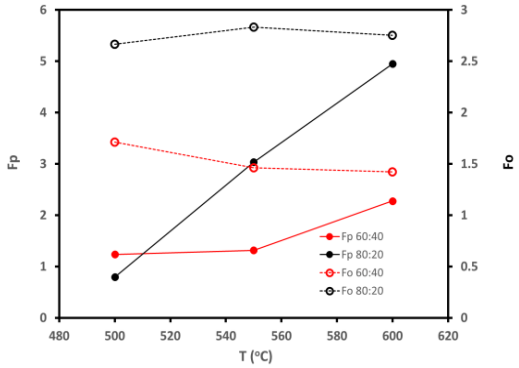

Fig. 5. Promotion factors F_p and F_o vs. testing temperature

CONCLUSION

It was demonstrated that the anode microstructure can be successfully nano-engineered by inkjet printing infiltration. The IJP infiltration enabled high precision permeation of the GDC sol ink allowing formation of GDC percolative nano-decoration on the anode scaffolds. As modified anode scaffolds showed significant enhancement of their electrochemical performance with the activation polarization improvement factor for 8 infiltration/heating cycles reaching $F_p = 4.95$ which led to equalization of the performances for both anode compositions.

Acknowledgements: *The authors wish to acknowledge EPSRC-UK grant (EP/M014304/1) - "Tailoring of microstructural evolution in impregnated SOFC electrodes" for the financial support.*

REFERENCES

1. N.H. Menzler, F. Tietz, S. Uhlenbruck, H.P. Buczzhkremer, D. Stöver, *J. Mater. Sci*., **45**, 3109 (2010).
2. S.P. Jiang, S.H. Chan, *J. Mater. Sci*.,*39*, 4405 (2004).
A. Weber, E.Ivers-Tiffee, *J. of Power Sources*, **127**, 273 (2004).
3. I.R. Gibson, G.P.Dransfield, and J.T. Irvine, *J. Eur. Ceram. Soc*., **18**, 661 (1998).
4. S. Singhal S,, *Solid State Ionics*, **135**, 305 (2000).
5. S.P.S. Badwal, S.Giddey, C.Munnings, A. Kulkarni,*J. of the Australian Ceramics Soc*., **50**, 23(2014).
6. S.P. Jiang, S.H. Chan, *J. Mater. Sci*., **39**, 4405(2004).
7. R.I. Tomov, M.Krauz, J.Jewulski, S.C. Hopkins, J. R. Kluczowski, D. M. Glowacka, B. A. Glowacki, *J.of Power Sources*,**195**, 7160 (2010).
8. Ch.Wang, S. C. Hopkins, R. I. Tomov, R.V. Kumar, B. A. Glowacki, *J. of the European Ceramic Soc*.,**32**, 2317 (2012)
9. Wang, Ch., Tomov, R.I., Kumar, R.V., Glowacki, B.A., *J. of Materials Science*, **46**, 6889 (2011).
10. A.M. Sukeshini, R. Cummins, T.L. Reitz, R.M. Miller, *J. Am. Ceram. Soc*., **92**, 2913 (2009).
11. K.T. Lee, H.S. Yoon, J. S. Ahn and E. D. Wachsman, *J. Mater.Chem*., **22**, 17113(2012).
12. J.L.M. Rupp, A.Infortuna, L.J. Gauckler, *Acta Materialia*, **54**, 1721(2006)

ПРИЛОЖЕНИЕ НА МАСТИЛЕНО-СТРУЙНОТО ПРИНТИРАНЕ ПРИ ИЗГОТВЯНЕ И МОДИФИКАЦИЯ НА АНОДИ ЗА ТВЪРДОТЕЛНИ ГОРИВНИ КЛЕТКИ

Р.И. Томов[1*], А. Факее[1], ТТ.Б. Митчел-Уилямс[1], М. Крауз[2], Р.В. Кумар[1], В.А. Гловацки[1,3]

[1] Department of Materials Science and Metallurgy, University of Cambridge, United Kingdom
[2]Institute of Power Engineering - Ceramic Department CEREL, Poland
[3] Institute of Power Engineering, Warsaw, Poland

Постъпила на 25 септември, 2017г.; Приета на 17 октомври 2017 г.
(Резюме)

Изследвана бе приложимостта на мастилено-струйното принтиране при изготвяне и модификация на твърдотелни горивни клетки. Мастилено-струйното принтиране във неговия вариант "Капка при поискване" предлага бърз, лесно мащабируем и икономически ефективен път за производство осигурявайки репродуктивно генериране на капки с обем между нано-литър до пико-литър с висока честота (*kHz*) и скорост (*1-10 m/*s). Елекромагнитни печатни глави бяха използвани за генерация на капки от различни мастила (допиран цериев окис, никелов окис) при поискване. Принтиращи параметри като налягане и време за отваряне на дюзата бяха изследвани с цел оптимизация на генерацията и доставката на капки. Преследвано бе намаляването на поляризационните загуби в анода на твърдотелната клетка чрез нано инженерство на скелета на електрода. Беше приложен метод на принтиране в две стъпки. Първоначално бе създаден порист електроден скелет от Gd:CeO_2-NiO. Във следващия етап нано декорация на електродния скелет бе постигната с контролирано принтиране на Gd:CeO_2. Така изработените симетрични анодни клетки бяха изследвани с Електрохимична Импедансна Спектроскопия с цел разкриване на връзката между повърхностната нано структура и електрохимичната активност. Данните от измерванията с Електрохимичната Импедансна Спектроскопия потвърдиха значително намаляване и сближаване на стойностите на ареалното специфично съпротивление на инфилтрираните аноди характеризирани с различно обемно съотношение на NiO/Gd:CeO_2. Настоящото изследване демонстрира възможността за постигане на значително подобрение на активността на твърдотелните горивни клетки чрез използване на проста индустриално мащабируема процедура.

Ключови думи: мастилено-струйното принтиране, инфилтрация, нано декорация, допиран цериев окис